L. SOZAŃSKA-JĘDRASIK*#, J. MAZURKIEWICZ*, W. BOREK*, K. MATUS*,
B. CHMIELA**, M. ZUBKO***

EFFECT OF Nb AND Ti MICRO-ADDITIVES AND THERMO-MECHANICAL TREATMENT OF HIGH-MANGANESE STEELS WITH ALUMINIUM AND SILICON ON THEIR MICROSTRUCTURE AND MECHANICAL PROPERTIES

The results are based on two experimental high-manganese X98MnAlSiNbTi24-11 and X105MnAlSi24-11 steels subjected to thermo-mechanical treatment by hot-rolling on a semi-industrial processing line. The paper presents the results of diffraction and structural studies using scanning and transmission electron microscopy showing the role of Nb and Ti micro-additives in shaping high strength properties of high-manganese austenitic-ferritic steels with complex carbides. The performed investigations of two experimental steels allow to explain how the change cooling conditions after thermo-mechanical treatment of the analysed steels affects the change of their microstructure and mechanical properties. The obtained results allow assessing the impact of both the chemical composition and the applied thermo-mechanical treatment technology on the structural effects of strengthening of the newly developed steels.

Keywords: high-manganese steels, TRIPLEX, microstructure, κ carbides, M_7C_3, EBSD, Nb and Ti micro-additives, grain size.

1. Introduction

The subject of this work is the study of high-manganese steels with reduced density obtained due to the relatively high aluminium content, which is currently included in some of the promising grades of structural steels (Fig. 1). Although the high-manganese steels are known for more than 130 years due to R. Hadfield's idea have a specific application, for a dozen or so years they have been experiencing a great interest of scientists around the world as a future construction material. The pursuit of ever higher and more complicated constructions with a high volume fraction of steel is connected with the requirement to use such steel grades for their construction, which, without heat treatment, allow obtaining high values of strength and impact resistance while maintaining good plastic properties. The key here is also the ability to obtain ready-made bars, tubes and profiles by thermo-mechanical treatment to obtain a structural material with a strength and yield strength exceeding 1000 MPa.

At the Institute of Engineering Materials and Biomaterials, Silesian University of Technology have been carried out extensive investigations of newly-developed high manganese austenitic steels have been carried out since 2013 what was confirmed and already published in many international scientific studies [1-5].
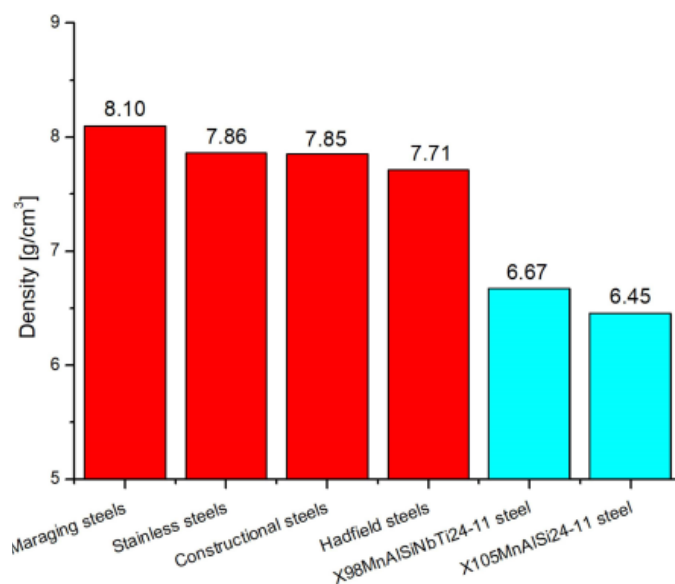

Fig. 1. Comparison of the density of various structural steels [2]

Designed for this purpose steels have been produced on a laboratory scale and subjected a multi-aspect analysis of the influence of thermo-mechanical treatment on their microstructure and mechanical properties. As base considerations,

* SILESIAN UNIVERSITY OF TECHNOLOGY, INSTITUTE OF ENGINEERING MATERIALS AND BIOMATERIALS, 18A KONARSKIEGO STR., 44-100 GLIWICE, POLAND
** SILESIAN UNIVERSITY OF TECHNOLOGY, INSTITUTE OF MATERIALS SCIENCE, FACULTY OF MATERIALS ENGINEERING AND METALLURGY, 8 KRASINSKIEGO STR., 40-019 KATOWICE, POLAND
*** UNIVERSITY OF SILESIA, INSTITUTE OF MATERIALS SCIENCE, 1A 75 PUŁKU PIECHOTY, 41-500 CHORZÓW, POLAND
# Corresponding author: liwia.sozanska-jedrasik@polsl.pl

scientific developments introduced two steels: one with the micro-additives of Nb (0.048%), and Ti (0.019%) and the other with the identical composition but without the micro-additives. Steels of this type are still in the phase of research and scientific analysis and reports of possible attempts of industrial use practically negligible [6-10]. Answering the question why just these two micro-additives were used as microstructure modifiers, and thus the properties of the studied group of steel are based on the extensive experience of the team performing the studies. An in-depth analysis of the impact of Nb and Ti on the properties of the this and other groups of structural steels gives additional cognitive knowledge in a new possibility of their applications. Universality and availability of this type of micro-additives in industrial use is their additional asset [11-13]. The use of Nb and Ti as elements essential for the analysis of changes in the properties of steel in this group are also related to their beneficial effect on the maintenance of fine-grained microstructure, which is the basis of good mechanical properties of materials and analysis of morphology and strength of Nb and Ti carbides in such group of steels. The research results presented in this paper are not yet a comprehensive assessment of the impact of Nb and Ti on the microstructure and properties of this group of steels as it is ultimately planned, but they already gave a chance to learn the direction and strength of their impact. It is interesting all the more that during the thermo-mechanical treatment is not noticed so far the effects of precipitation associated with these micro-additives bound in carbides [14-16].

The high-manganese TRIPLEX type steels analysed in this work are characterized by a multiphase microstructure composed of γ-Fe austenite (Mn, Al, C), α-Fe ferrite (Mn, Al) and carbides precipitate, including κ-(Fe, Mn)$_3$AlC, which is key for their properties. [17-20]. The mechanical properties of high-manganese steels are highly dependent on the location, size and morphology of the carbides κ-(Fe, Mn)$_3$AlC. These carbides can also be the cause of the brittleness of steel during plastic deformation at room temperature when are formed at the grain boundaries [6,7,21]. The key to the mechanical properties of this group of high-manganese steels is the method of carrying out thermo-mechanical treatment, which is a beneficial method of producing mass products in economic terms. A well-designed thermo-mechanical treatment can increase the strength of the material while maintaining its ductility at a good level [22-27].

2. Experimental (materials and methods)

The subject of the work is the researches two experimental high-manganese TRIPLEX type steels developed at the Silesian University of Technology in Gliwice, X98MnAlSiNbTi24-11 (X98 steel) and X105MnAlSi24-11 (X105 steel), whose detailed chemical compositions obtained on the basis of melting analysis

Chemical composition newly developed high-manganese steels (wt.%)

Elements	C	Mn	Al	Si	Nb	Ti	Ce	La	Nd	P$_{max}$	S$_{max}$
Steel X98MnAlNbTi24-11											
[wt. %]	0.98	23.83	10.76	0.20	0.048	0.019	0.029	0.006	0.018	0.002	0.002
Steel X105MnAlSi24-11											
[wt. %]	1.05	23.83	10.76	0.10	—	—	0.037	0.011	0.015	0.005	0.005

are presented in Table 1. The methodology of obtaining the material for the research including the description and parameters of forging and rolling has been presented in earlier works [2,5,22]. This publication presents only the most important information allowing for an orientation as to the scope and method of thermo-mechanical treatment of the analysed steels.

Steels were melted in a laboratory vacuum induction furnace the batch weight 25 kg and cast in an argon atmosphere into a cast iron ingot (Φ145 mm/h = 200 mm). After cooling in the air, a hot plastic treatment was made using a free forging method on a high-speed hydraulic press, for flat bars with a thickness of approx. 20 mm. The forging temperature was in the range from 1200 to 900°C with in-process heating, so that the material did not cool down below 900°C. Test sections of examined steels with dimensions 5×185×600 mm were subjected to the hot-rolling. The batch was austenitized at 1150°C for 15 min. The material was subjected to a four-stage rolling on a single-groove double-roll mill with a roll diameter of 550 mm, with a linear speed of 0.74 m/s in the temperature range from 1100°C to 850°C with a 0.23 strain for each passes. A detailed diagram of the rolling process is shown in Figure 2. After the last rolling pass, the sheet of steels were cooled in three variants: in water; in the air and 30s; and isothermal heating at temperature of last stage of hot-rolling and cooling in water, obtaining a flat sheet of steels 210 mm wide and approx. 3.2 mm thick.

Samples for structural studies using light microscopy and scanning electron microscopy were included, and then ground and mechanically polished on abrasive papers and discs moistened with diamond suspension, ending the polishing process with a diameter smaller than 1 μm. To reveal the microstructure as a reagent, a 5% solution of HNO$_3$ in ethyl alcohol was used. The specimens for diffraction examinations by EBSD technique in a scanning electron microscope were ground with a grinder-polisher with sandpapers and then polished electrochemically in a reagent with the following composition:
- 950 ml of 99% hydrochloric acid (CH$_3$COOH);
- 50 ml of 60% tetraoxochloric acid (HClO$_4$).

Observations of the microstructure of the investigated steels were carried out using the Axio Observer light microscope from Zeiss. Research using the SUPRA 35 scanning electron microscope from Zeiss was carried out at 15 kV acceleration using secondary electron detection (SE). An EDS detector and a camera for diffraction tests connected to the above microscope in Trident XM4 system by Edax were used to examine the chemical and phase composition of the specimen micro areas and precipitates and particles. EBSD research was carried out at the accelerating
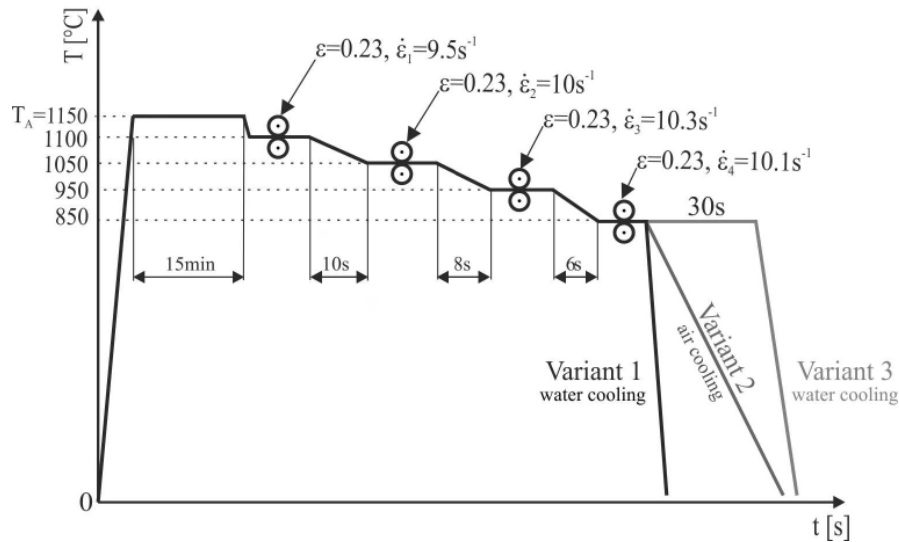
Fig. 2. Diagram of the actual hot-rolling process with different cooling variants

voltage of 20 kV, the working distance of 15 mm and step size of 0.20 μm.

The samples for structural examinations in transmission electron microscope (TEM) have been cut, then TEM samples were prepared by mechanical grinding the specimens to a thickness of 60 μm and ion beam polishing. Transmission electron microscope studies were conducted at the accelerating voltage of 300 kV. TEM investigations were performed in a probe Cs-corrected S/TEM Titan 80-300 FEI microscope. Selected area electron diffraction patterns were obtained with a camera length of 215-330 and condenser aperture C2-50.

The aim of the conducted research was to analyse changes in the microstructure and mechanical properties of X98 steel with micro-additives and reference to X105 steel without these additives after thermo-mechanical treatment (real hot-rolling of sheet steel sections) taking into account the influence of Nb and Ti micro-additives.

3. Results and Discussion

The first stage of the analysis of the microstructure of newly developed steels was analysis after forging, which already revealed the very strong structural diversification of the X98 and X105 steels (Fig. 3). Both examined steels are multiphase dominant share an austenitic microstructure which is particularly noticeable in the steel with Ti and Nb micro-additives and other phases like ferrite and varied in morphology and chemical composition of the carbides, as widely shown in other publications [1-3].

Analysing the microstructure of steels X98 and X105 after forging it was found that in steel containing Nb and Ti ferrite grains are evenly distributed at the grain boundaries of austenite. In X105 steel, it was noticed that ferritic areas are much longer and wider than in X98 steel and ferrite banding was noticed. Analysing the above test results, it can be concluded that Nb

and Ti micro-additions significantly influence the grinding of austenite and ferrite grains in the investigated steels. Research performed using diffraction in SEM so-called EBSD technique
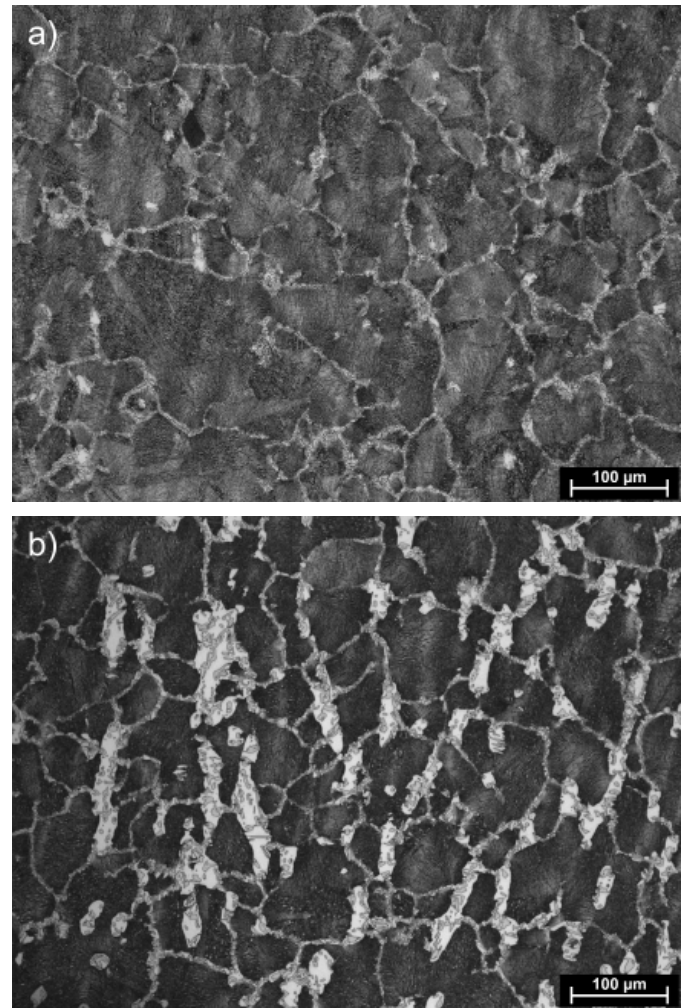

Fig. 3. A multiphase microstructure of the steel: X98 (a) and X105 (b) after forging

allows determining the distribution and location of individual components of the microstructure along with their size. It was found that the average diameter of austenite grain in this state is 42 μm and 62 μm respectively for X98 and X105 investigated steels. The X98 steel grain, which is about 32% smaller, is in line with expectations. Nb and Ti clearly affected the growth of the grain size at this technological stage of steel production. The volume fraction of ferrite in steel with additions of Nb and Ti (X98) is ~6% and in the case of reference X105 steel its share is up to 15% (Figs. 3). Such a significant difference in the volume fraction of ferrite is surprising and will it will definitely affect on the mechanical properties of investigated steels which will be tested in the next step. Based on the results of the EBSD technique in SEM, it can be concluded that both steels are dominated by wide-angle borders with a confusion angle of >15°, whose percentage is ~94%. Microhardness values for the ferrite in the investigated steels is slightly higher than microhardness values of austenite constituting the main phase component. The microhardness of ferrite and austenite is similar in both investigated steels and it is shown in figure 4.

The microstructure of the investigated steels varied considerably during the pre-treatment stage after a four-step hot-rolling with each pass equal 20% according to the parameters shown in figure 2 as shown in Figures 5 and 6 obtained from samples cut in the direction of rolling.

The thermo-mechanical treatment with three optional variants of cooling ordered the microstructures of both examined steels, and the initially visible differences significantly decreased, both morphologically and dimensionally. In the state after rolling, the volume fraction of ferrite in X98 steel is ~3%, while in X105 steel ~10%. The microstructures of both steels are austenite grains with numerous annealing and deformation twins. Ferrite occurs in the form of elongated grains in both steels, which is a characteristic feature of austenitic-ferritic microstructures and results from its low tendency to recrystallization. Such a ferrite morphology is favoured by a high aluminium content in the investigated steels. The ferrite bands are located in the micro-
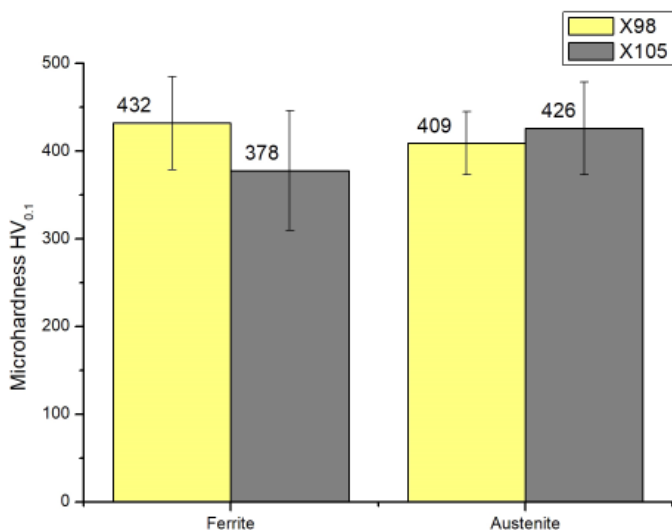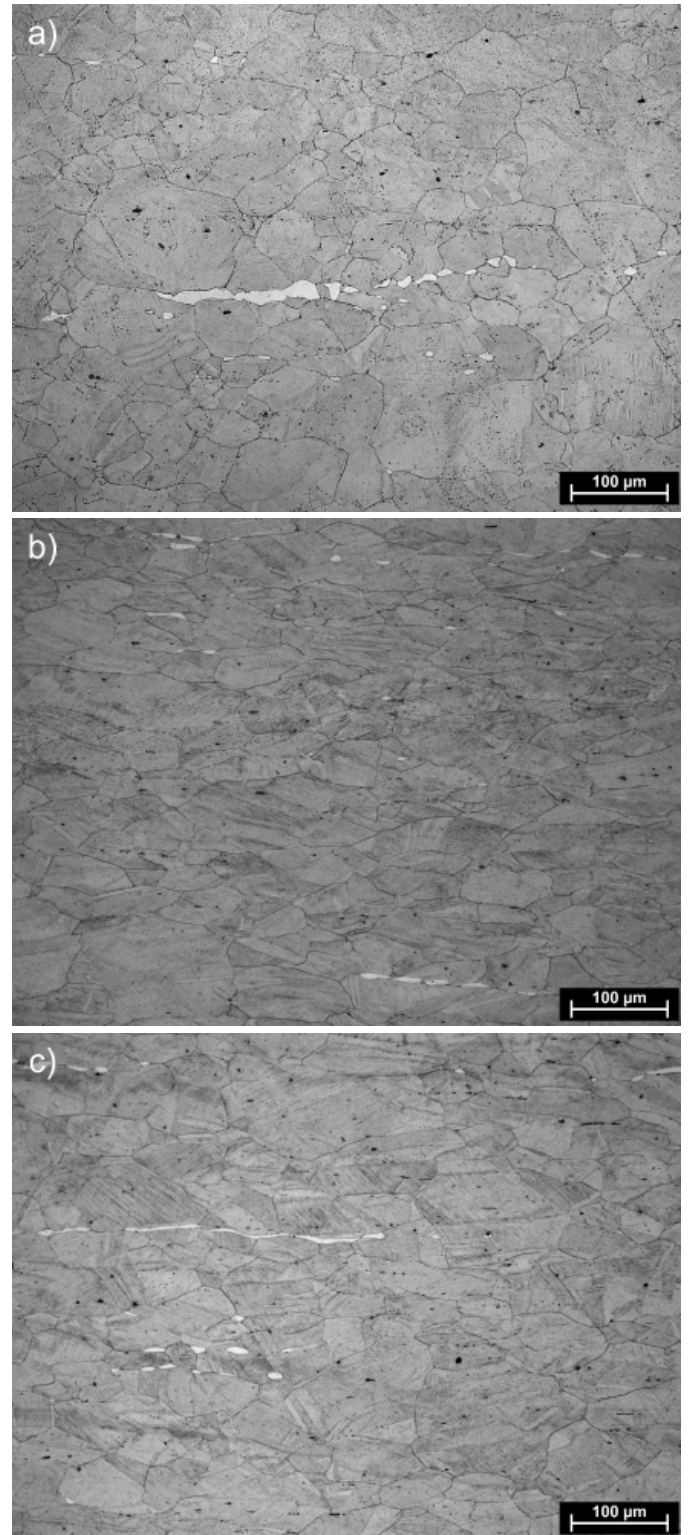

Fig. 5. Microstructure of X98 steel after four-stage hot-rolling and cooling acc. variant 1 (a), variant 2 (b), variant 3 (c)

Fig. 4. Comparison of average values of microhardness of $HV_{0.1}$ austenite and ferrite of investigated steels after forging

structure are parallel to the direction of rolling. In X98 steel, ferrite grains are 20% smaller than for X105 steel. The results of the EBSD technique show that the samples after hot-rolling are characterized by two main orientations with the direction [111] and [001], however the volume of grains oriented in the direction [111] parallel to the direction of hot-rolling (HRD) is greater and about 70% (Figs. 7a, 8a). There is a clear differ-
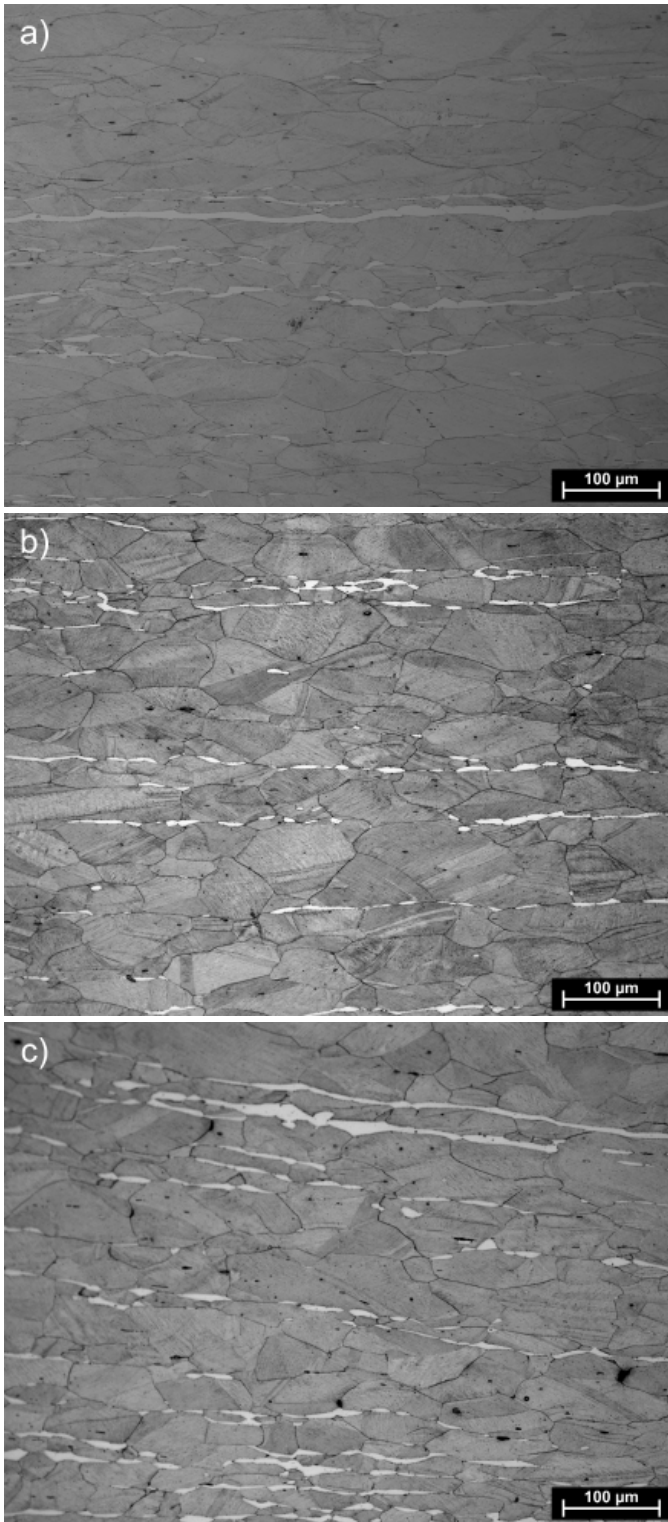
Fig. 6. Microstructure of X105 steel after four-stage hot-rolling and cooling acc. variant 1 (a), variant 2 (b), variant 3 (c)

ence in the ferrite content in both investigated steels. It is not as strong as it was after forging, but it has given much more ferrite to the steel microstructure without niobium and titanium micro-additives. In X98 steel, the volume fraction of ferrite is 3% (after forging 6%), while in X105 steel – 10% (almost 15% after forging). In the investigated steels, carbides are responsible for good mechanical properties, which in particular in steel with

Nb and Ti is much more quantitatively. Both in X98 and X105 steel, diffraction was found using an X-ray diffractometer [1] as diffractionally by the EBSD technique in SEM as presented in this article in figures 7 and 8 the presence of Mn_7C_3 carbide at the grain boundaries. Based on the above-mentioned EBSD tests, it was found that after all variants of cooling, wide-angle boundaries prevail in both investigated steels, with a percentage share of ~65% (Figs. 7c, 8c). A relatively large share of low-angle boundaries, with an angle of disorientation less than 15°, determines whether recrystallization in the analysed steels has come to an end. X98 steel after hot-rolling and cooling acc. variants presented in figure 2 is characterized by greater grain refinement than X105 steel, which is obviously related to the effect of Nb and Ti micro-additives.

During the research in SEM using the EDS technique, the chemical composition of carbides disclosed in the X98 and X105 steels microstructure were analysed both at the pre-treatment stage by forging and after four-stage rolling with three cooling variants. Of course, the carbide-forming micro-additions of Nb and Ti in X98 steel was caused the appearance in the microstructure of large numbers and volumes of carbides (Nb, Ti)C of a size from several dozen nanometres to several micrometres, what was not present in the X105 base steel. The high carbon content in these steels additionally enhanced the precipitation effects of carbides. In both the steels it was also disclosed M_7C_3-type carbides, and κ-(Fe, Mn)$_3$AlC carbides (Figs. 9,10). A detailed analysis of the fraction and morphology of the carbides of these steels are shown in [2,3]. Based on Nb and Ti carbides are released in austenite, ferrite and grain boundaries. At the grain boundaries in both steels also the AlN precipitation of 1 to 3 μm were noticed (Fig. 9). Niobium and titanium in X98 steel are bonded in carbides and more efficiently inhibit the growth of austenite grains. Carbides κ-(Fe,Mn)$_3$AlC in X98 and X105 steels were most commonly disclosed at grain boundaries. In X98 steel the size of κ carbides ranges from a few nanometres to approx. 160 nm, while in X105 steel both carbides with a size of several nanometres and up to 800 nm appear. This is probably also related to the different distribution of carbon in both investigated steels due to the higher content of carbide forming elements in X98 steel. It was also noticed during the carbide size tests that the analysed steels after air-cooling (variant 2 – Fig. 2) were characterized by considerably larger κ carbides sizes, which may be related to the cooling method after thermo-mechanical treatment.

Of course, one of the most interesting cognitively for the microstructure and analysis of structural mechanisms is research in the transmission electron microscope, which was carried out as part of this work. Studies using TEM provide an opportunity for a detailed analysis of network coherence precipitates (carbides) matrix and determination of parameters of a data network carbides and especially the smallest ones. It should be noted, however, that the preparation itself requiring a good carbide reduction while maintaining the matrix is a difficult task and requires a great deal of skill in the operator of the preparation equipment. The occurrence of κ carbides were confirmed using TEM in both investigated steels with a regularly face-centered
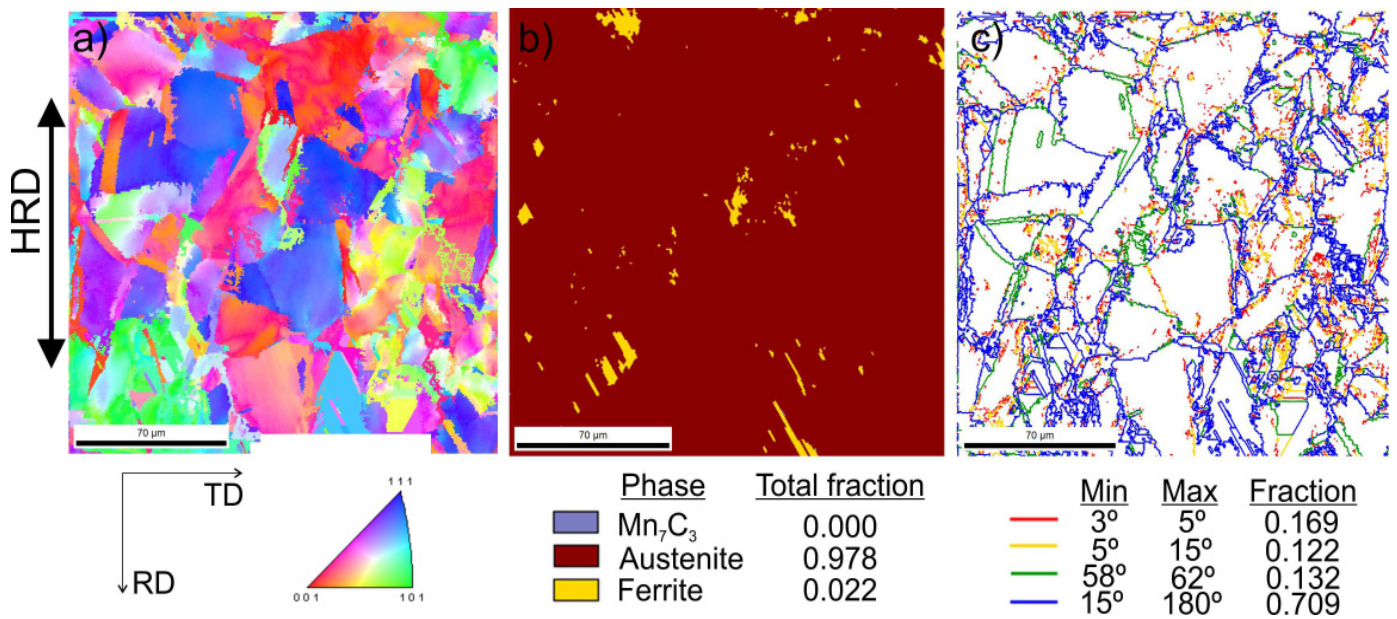
Fig. 7. Microstructure revealed by EBSD technique in SEM in the selected microarea of the investigated steel X98 after hot-rolling and cooling in air (variant 2): crystallographic orientation map(a), EBSD phase map (b), misorientation angles map (c)
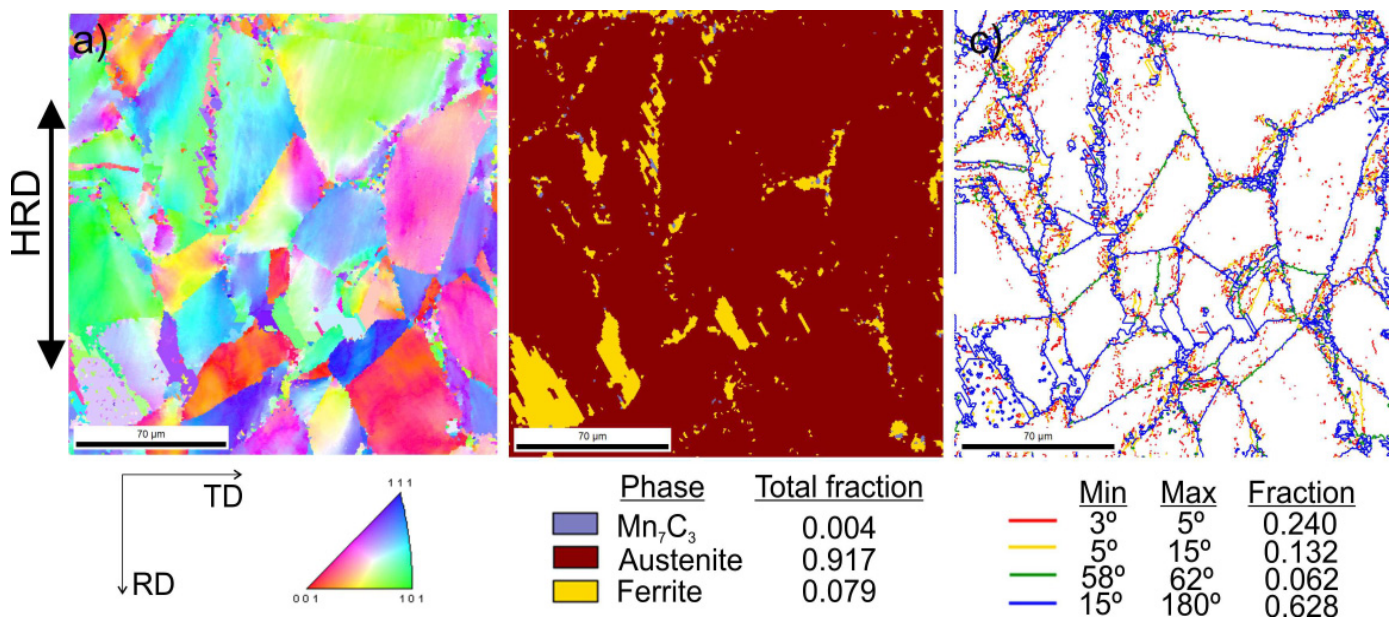

Fig. 8. Microstructure revealed by EBSD technique in SEM in the selected microarea of the investigated steel X105 after hot-rolling cooling in water (variant 1): crystallographic orientation map(a), EBSD phase map (b), misorientation angles map (c)

TABLE 2

Results of EDS spectrum analysis for areas from Fig. 9 (wt. [%])

Elements	Point 1	Point 2	Point 3	Area 4	Area 5
C*	8.9	12.2	8.0	15.9	10.3
Al	13.5	13.5	12.2	1.8	9.6
Nb	—	—	—	49.8	7.8
Ti	—	—	—	15.0	2.0
Mn	23.0	21.3	21.8	6.7	20.6
Fe	54.6	53.5	56.7	11.0	49.5

TABLE 3

Results of EDS spectrum analysis for areas from Fig. 10 (wt. [%])

Elements	Point 6	Point 7	Point 8
C*	4.1	8.7	10.1
N*	7.2	—	—
Al	40.5	13.8	13.1
Mn	13.8	23.1	23.5
Fe	34.3	54.3	53.3

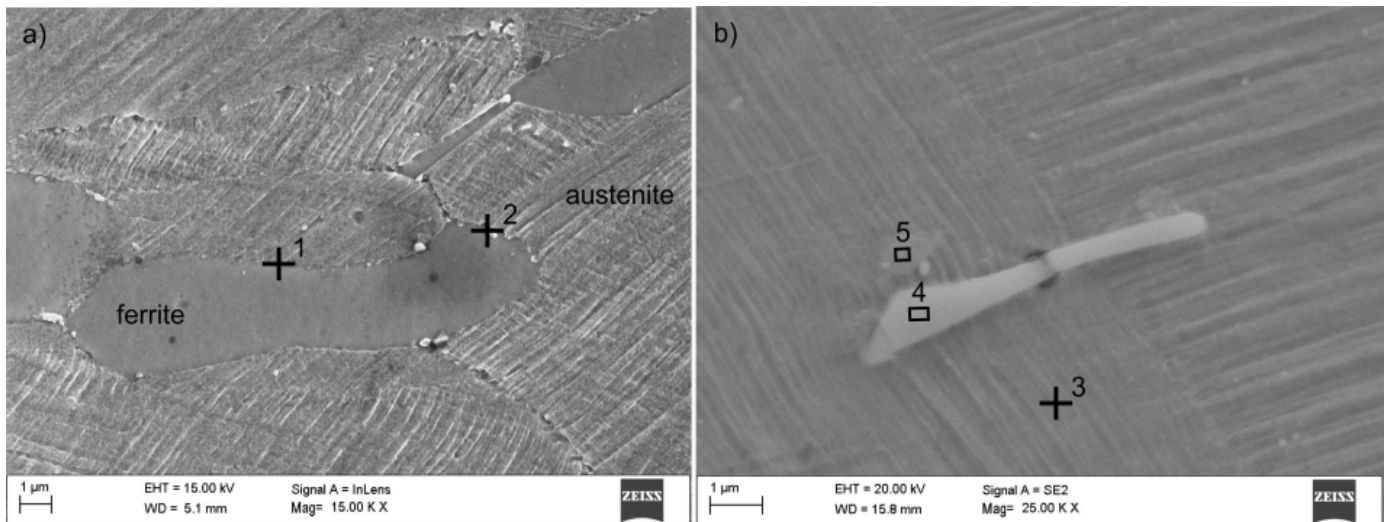*) the content of C and N is an approximate value due to the measurement method.

Fig. 9. Microstructure of X98 steel after hot rolling and cooling: acc. variant 2 (a), by variant 3 (b) with disclosed carbides together with measurement of chemical composition by EDS (SEM)
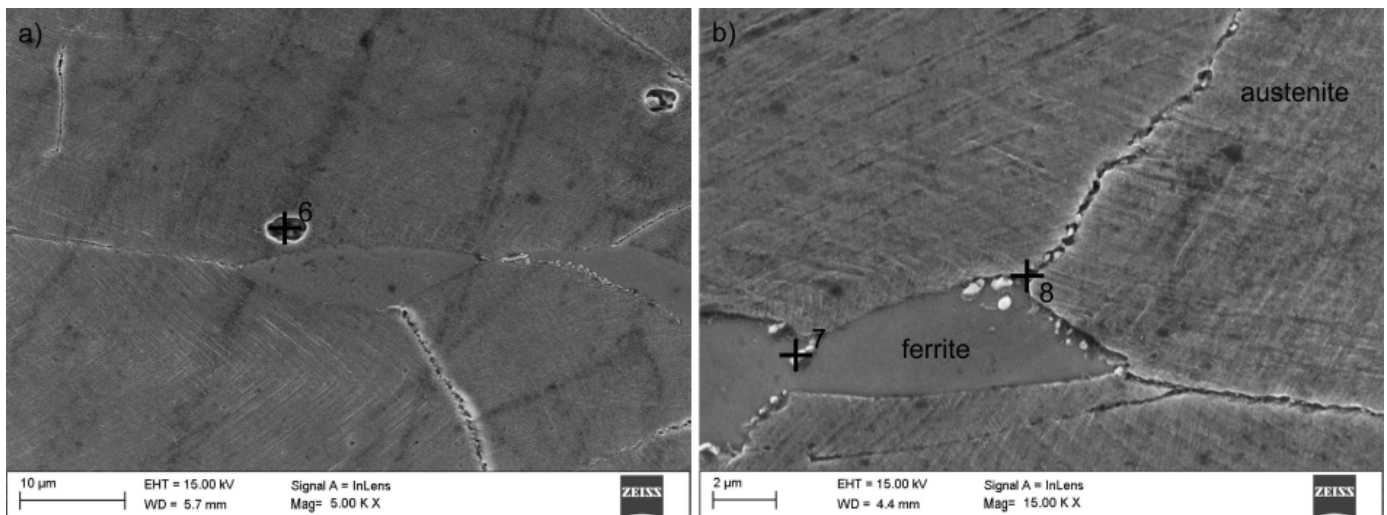

Fig. 10. Microstructure of X105 steel after hot rolling and cooling: acc. variant 3 (a), acc. variant 2 (b) with disclosed carbides and AlN together with the measurement of the chemical composition by the EDS technique (SEM)

cubic lattice (fcc) (Pm-3m group) and the lattice parameter $a = 0.3875$ nm (Fig. 11). In austenite, Mn_7C_3 carbides were identified in the investigated steels (Fig. 12), characterized by an orthorhombic crystal lattice (Pnma group) with lattice parameters $a = 0.4546$ nm, $b = 0.6959$ nm, $c = 1.197$ nm. Mn_7C_3 carbides, however, occur in both austenite and ferrite, and their size is usually from 100-600 nm.

The structural effects described above revealed during metallographic studies of the analysed X98 and X105 steels are also related to their mechanical properties. These steels, after a thermo-mechanical treatment designed in three variants (Fig. 2) differing in the final cooling method, show high strength properties, and as already indicated in [5] also a high value of yield stress, most often over 0.9 of the R_m value. Figure 13 presents a comparison of the values of tensile strength R_m and yield strength $R_{p0.2}$ determined in a static tensile test at the room temperature of investigated steels depending on the method (vari-

ant) of cooling after semi-industrial rolling. In the next figure (Fig. 14), the change of the relative elongation (A) of the investigated steels for the above-mentioned machining variants was presented analogously to R_m and $R_{p0.2}$. Analysing these results, it was found that the highest strength properties ($R_m = 1142$ MPa) are obtained steadily with Nb and Ti micro-additives in Variant A after cooling in water. In other variants, the strength is for X98 steel is slightly smaller, and taking into account the number of samples for research and the obtained detailed values, statistical analysis showed the lack of significance of differences at this level. It can therefore be assumed that the method of termination of the thermo-chemical treatment (the cooling variant) is not of significant importance for the obtained strength properties of this steel. The results defining the yield point values for X98 steel must be interpreted somewhat differently. Here it can be seen for $R_{p0.2}$ marked decrease its value (approx. 16%), which may be related in part to the above-described phenomenon of growth of
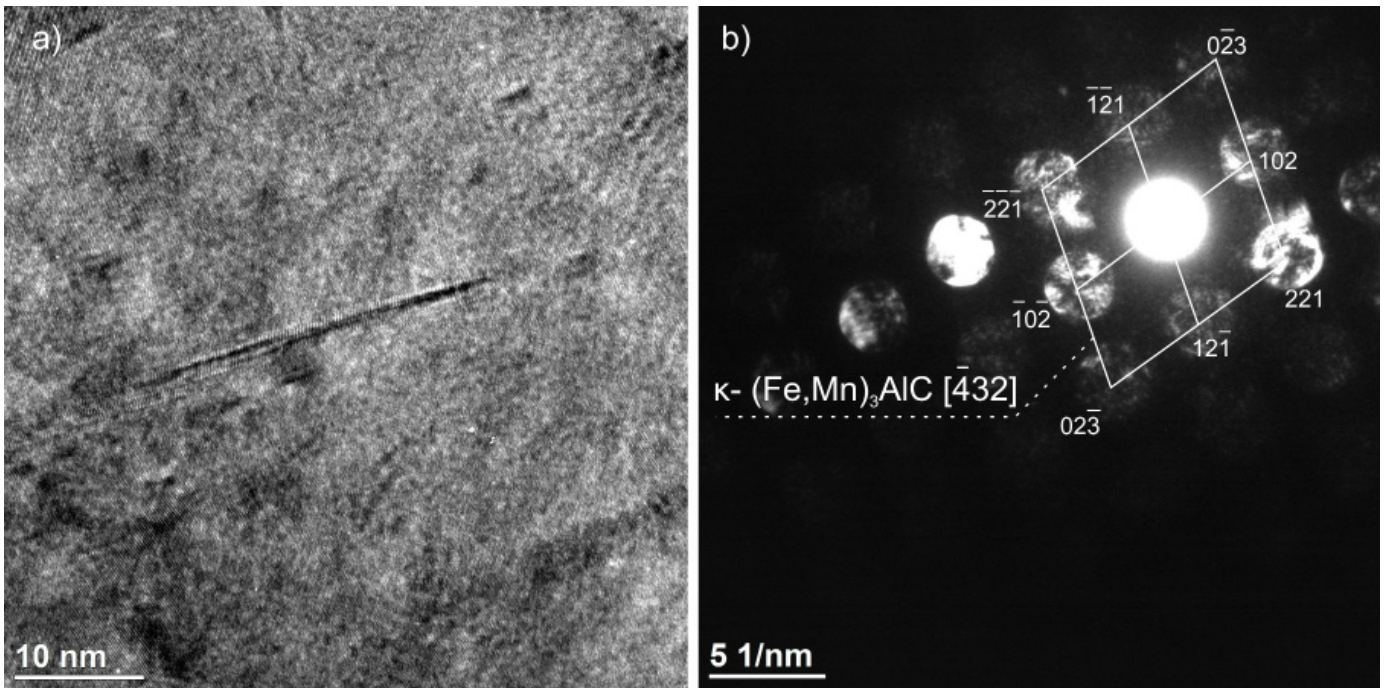
Fig. 11. HRTEM image of the X98 steel precipitates κ carbide (a), nano diffraction pattern of the zone axis $[\bar{4}32]$ κ (b)
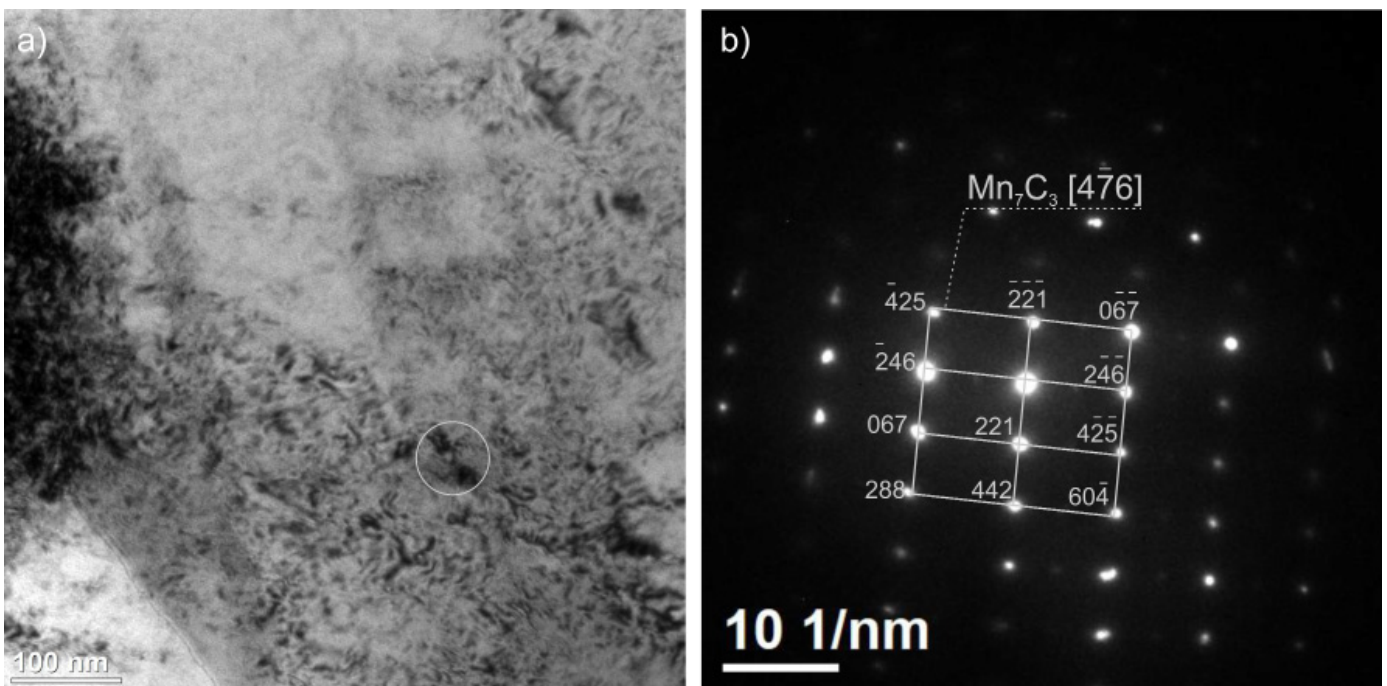

Fig. 12. Precipitation Mn_7C_3 carbide in austenite – X105 steel: bright field image (a), diffraction pattern of the zone axis $[4\bar{7}6]$ Mn_7C_3 (b)

carbides κ for this variant of cooling after rolling. For X105 steel, tensile strength as well as yield strength are slightly higher for almost all variants than for X98 steel. These differences are not exceeding 7.5% of the maximum value so they have no practical significance, nonetheless surprising. Currently, research works are carried out to determine the impact strength of the analysed steels, but due to the availability of material in the form of sheets with a thickness of approx. 3mm, these will be comparative tests (non-standard samples). The results of these studies will be published shortly, however based on preliminary tests was found that impact values can definitely show one of the investigated steel in a bad light. The results of plastic properties tests are correlated concerning the values of strength and yield strength. In addition to variant 1, in the others variants can see lower values of plastic properties of investigated steels, especially where higher values of strength properties were obtained. It can be noticed when analysing figure 15 that for X105 steel plastic properties decrease for each subsequent cooling variant reaching

a minimum value of 22% elongation in the variant 3. In turn for X98 steel the tendency of change in elongation is opposite to that of the base steel reaching the highest extension value for variant 3 amounting to 28%.

4. Conclusion

Based on the results of experimental studies of two high-manganese steels X98MnAlSiNbTi24-11 (X98) and X105MnAlSi24-11 (X105) obtained and presented in this work, the following conclusions were made:

- In a microstructure after forging of steel containing Nb and Ti ferrite grains are evenly distributed over the boundaries of austenite grains. In X105 base steel it was noticed that ferritic areas are much longer and wider than in X98 steel and their banding was found. Three types of carbides have also been identified in the microstructure of both steels. The volume fraction of ferrite in X89 steel is ~6%, while in X105 ~15%. The average size of austenite grain in X98 steel is 42 μm, while 62 μm in X105 steel. This indicates that the addition of Nb and Ti significantly affect the grinding of austenite and ferrite grain in the both investigated steels;

- The microstructure of X98 steel after hot-rolling is characterized by higher grain refinement compared to X105 steel, which is caused by the Nb and Ti micro-addition. These micro-additives create a dispersion particle of nitrides, carbonitrides and carbides with a regular network during hot plastic deformation, limiting the grain growth of recrystallized austenite. A characteristic feature of the austenitic-ferritic microstructures analysed are elongated ferrite grains, which results from a low tendency to recrystallize them. In addition, the content of aluminium in the investigated steels affects the formation of ferrite bands parallel to the rolling direction. In X98 steel, ferrite grains are 20% smaller than for X105 steel. In X98 steel, the volume fraction of ferrite is 3%, while in X105 – 10%.

- Based on EBSD investigation it has been found that in both investigated steels dominate the wide-angle boundaries (misorientation angle $\theta \geq 15°$). There are also deforma-
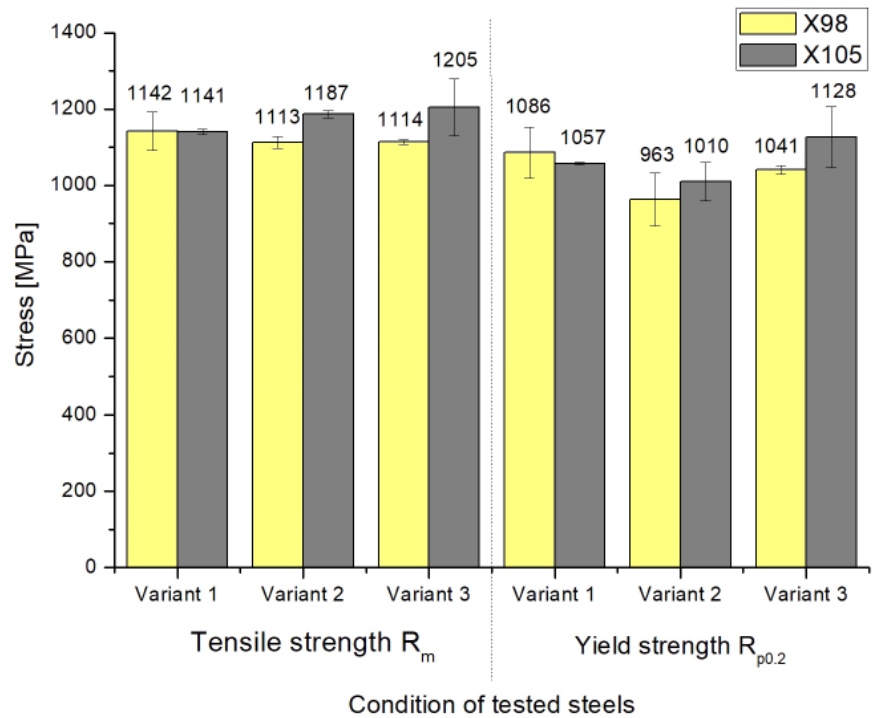

Fig. 13. The effect of the cooling variant after the thermo-mechanical treatment (hot-rolling) of the analysed steels on their tensile strength and the yield stress of the static determined tensile tests at ambient temperature
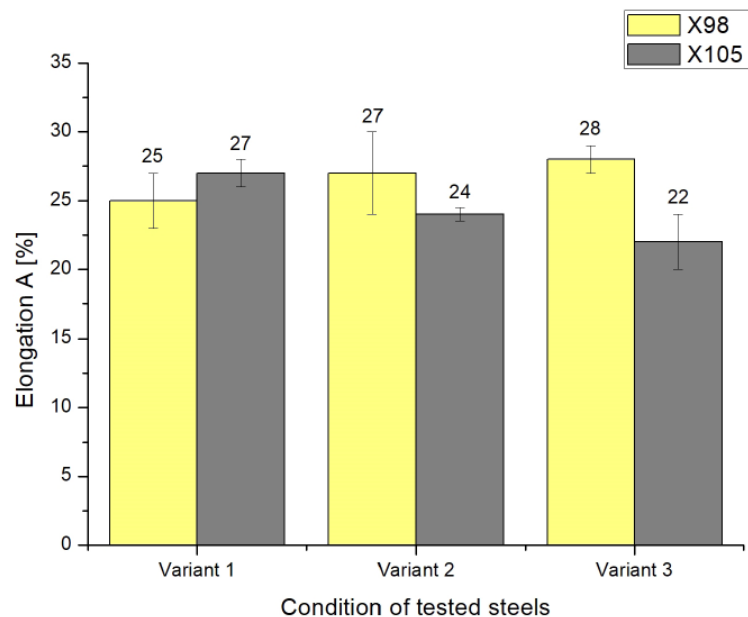

Fig. 14. Influence of the cooling variant after the thermo-mechanical treatment (hot-rolling) of the analysed steels on the value of their relative elongation determined during the static tensile test at ambient temperature

tions twins with a 58-62° deflection angle, while in X98 steel their share is greater by about 45% than in X105 steel. About 30% of the share of low-angle borders (misorientation angle $\theta < 15°$) in both studied steels may indicate that the recrystallization process has not been completed.

- Tests carried out with scanning and transmission electron microscopy of X98 steel revealed the presence of complex

carbides based on Nb and Ti in both austenite and ferrite. These carbides also locate at the grain boundaries, their size ranges from a few nanometres to 15 μm. Examination of the microstructure of X98 and X105 steels in transmission electron microscopy were allowed the identification of M_7C_3 type carbides and κ-(Fe, Mn)$_3$AlC carbides. The κ carbides in both investigated steels have a face-centered cubic lattice (fcc) (Pm-3m group) and the lattice parameter $a = 0.3875$ nm. In austenite in the investigated steels, Mn_7C_3 carbides were identified, characterized by orthorhombic crystal lattice (Pnma group) with lattice parameters $a = 0.4546$ nm, $b = 0.6959$ nm, $c = 1.197$ nm

Both investigated steels after thermo-mechanical treatment designed in three variants differing in the method of the final cooling show high strength properties above 1100 MPa, as well as a high value of yield point being the most frequently over 0.9 of the R_m value. Differences in tensile strength in individual cooling variants for X98 steel are negligible, and for X105 steel they do not exceed a few percents. Significantly lower values of the yield point were obtained for both investigated steels in the cooling variant in the air after thermo-mechanical treatment. These steels have relatively good plastic properties ranging from 22-28% depending on the cooling variant after the thermo-mechanical treatment.

REFERENCES

[1] L. Sozańska-Jędrasik, J. Mazurkiewicz, W. Borek, M. Kraus, METAL 2018, 855-860 (2018). ISBN 978-80-87294-84-0.

[2] L. Sozańska-Jędrasik, J. Mazurkiewicz, W. Borek, L.A. Dobrzański, Mater. Eng. **225** (5), 184-191 (2018). DOI 10.15199/28.2018.5.4

[3] L. Sozańska-Jędrasik, J. Mazurkiewicz, W. Borek, L.A. Dobrzański, Mater. Eng. **38** (2), 69-76 (2017).

[4] L. Sozańska-Jędrasik, J. Mazurkiewicz, W. Borek, Topical Issues of Rational Use of Natural Resources, 235-241 (2018). ISBN: 978-0-367-02743-8.

[5] L. Sozańska-Jędrasik, J. Mazurkiewicz, W. Borek, MATEC Web of Conferences, CMES'18. 252, 08005 (2019). https://doi.org/10.1051/matecconf/201925208005

[6] S. Chen, R. Rana, A. Haldar, R.K. Ray, Prog. Mater. Sci. **89**, 345-391 (2017).

[7] M. Bausch, G. Frommeyer, H. Hofmann, E. Balichev, M. Soler, M. Didier, L. Samek, Final Report RFCS Grant No. RFSR-CT-2006-00027 (2013).

[8] D.T. Pierce, J.A. Jiménez, J. Bentley, D. Raabe, J.E. Wittig, Acta Mater. **100**, 178-190 (2015).

[9] L. Zhang, R. Song, C. Zhao, F. Yang, Y. Xu, S. Peng, Mater. Sci. Eng. A **643**, 183-193 (2015).

[10] A. Etienne, V. Massardier-Jourdan, S. Cazottes, X. Garat, M. Soler, I. Zuazo, X. Kleber, Metall. Mater. Trans. A **45**, 324-334 (2014).

[11] A. Grajcar, Thermodynamic analysis of precipitation processes in Nb-Ti-microalloyed Si-Al TRIP steel, J. Therm. Anal. Calorim. **118** (2), 1011-1020 (2014).

[12] M. Opiela, Arch. Metall. Mater. **59** (3), 1181-1188 (2014).

[13] L.A. Dobrzański, W. Kasprzak, A. Zarychta, M. Ligarski, J. Mazurkiewicz, J. Mater. Process. Technol. **64** (1-3), 93-99 (1997).

[14] H. Zhang, D. Ponge, D. Raabe, Mater. Sci. Eng. A **610**, 355-369 (2014).

[15] S.S. Sohn, H. Song, B.C. Suh, J.C. Suh, J.H. Kwak, B.J. Lee, N.J. Kim, S. Lee, Acta Mater. **96**, 301-310 (2015).

[16] A.J. Craven, K. He, L.A.J. Garvie, T.N. Baker, Acta Mater. **48,** 3857–3868 (2000)

[17] J. Moon, S.-J. Park, J.H. Jang, T.-H. Lee, C.-H. Lee, H.-U. Hong, D.-W. Suh, S.H. Kim, H.N. Han, B.H. Lee, Scripta Mater. **127**, 97-101 (2017).

[18] O.A. Zambrano, J. Valdés, Y. Aguilar, J.J. Coronado, S.A. Rodríguez, R.E. Logé, Mater. Sci. Eng. A **689**, 269-285 (2017).

[19] M.J. Yao, P. Dey, J.-B. Seol, P. Choi, M. Herbig, R.K.W. Marceau, T. Hickel, J. Neugebauer, D. Raabe, Acta Mater. **106**, 229-238 (2016).

[20] L.N. Bartlett, D.C. Van Aken, J. Medvedeva, D. Isheim, N.I. Medvedeva, K. Song, Metall. Mater. Trans. A 45, 2421-2435 (2014).

[21] D. Liu, M. Cai, H. Ding, D. Han, Mater. Sci. Eng. A **715**, 25-32 (2018).

[22] W. Borek, T. Tański, Z. Jonsta, P. Jonsta, L. Cizek, METAL 2015: 24th International Conference On Metallurgy And Materials, 307-313 (2015).

[23] T. Tański, P. Snopiński, W. Borek, Mater. Manufact. Processes **32** (12), 1368-1374 (2017).

[24] L.A. Dobrzański, A. Grajcar, W. Borek, Mater. Sci. Forum **368**, 3224-3229 (2010).

[25] L.A. Dobrzański, W. Borek, J. Mazurkiewicz, Materialwiss Werkst. **47** (5-6), 428-435 (2016).

[26] L.A. Dobrzański, W. Borek, J. Mazurkiewicz, Arch. Metall. Mater. **61** (2), 725-730 (2016).

[27] S. Ebied, A. Hamadan, W. Borek, M. Gepreel, A. Chiba, Mater. Charact. **139**, 176-185 (2018).